QUANTUM DOT PHYSICS

Muminov Islamjon Arabboyevich
Fergana State University, Physics and Mathematics
doctor of philosophy (PhD); ima220790@mail.com
Sobirova Dilnoza Davlatjon qizi
Academic Lyceum of Fergana Polytechnic Institute
teacher of physics

Abstract: Quantum dots (QDs) have emerged as promising candidates for applications in lighting, energy, and bio-fluorescent detection due to their unique size-dependent properties. The photo physics of QDs is primarily governed by the size of the nanoparticles, although the influence of ligand schemes and shells has been recognized as significant. This chapter provides a comprehensive overview of different QD models, beginning with the fundamental "particle-in-a-box" model and progressing to more advanced and intricate models employed for quantifying QD photo physics. The discussion delves into the intricate interplay between QD size, ligand configurations, and shell architectures, elucidating their effects on the optical properties of QDs. By understanding these models, researchers can gain insights into the design and optimization of QDs for various applications, thus paving the way for enhanced performance and efficiency in lighting, energy generation, and bio-fluorescent detection systems.

Keywords: Quantum dots, Size-dependent properties, Lighting applications, Energy applications, Bio-fluorescent detection, Photo physics, Nanoparticles, Ligand schemes, Shell architectures, Particle-in-a-box model, Quantum dot models, Optical properties, Size effects, Ligand impact, Photo physics quantification.

1. Introduction.

The size dependent properties of quantum dots make them great candidates for applications in lighting, energy, and bio-fluorescent detection. On the most basic level, the size of the nanoparticles plays the largest role in their photo physics, yet various ligand schemes and shells have been shown to have a considerable impact on their photophysics. This chapter will discuss various quantum dot models, starting with the most basic, "a particle-in-a-box", and then moving on to the more sophisticated and technical models that are used to quantify quantum dot photophysics.
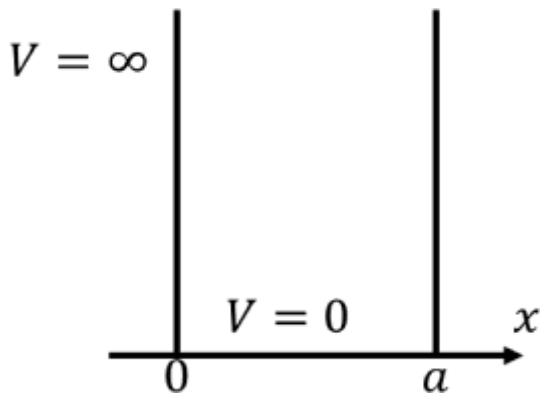
Particle-in-a-Box

Figure 1. Model of a particle-in-a-box with infinite potentials outside the box and zero potential inside.

The particle-in-a-box model is one of the simplest applications of the Schrödinger equation, but it can portray one the most import aspects of quantum dot physics; the size dependent band gap. In this model, one assumes that an electron is bound to its nucleus, trapped inside a box of length a. An infinite potential ($V = \infty$) exists outside of the box while there is no potential ($V = 0$) inside of the box (Figure 1). The Schrödinger equation for this example can be written as

$$\frac{d^2\psi}{dx^2} + \frac{2m}{\hbar^2}E\psi = 0 \qquad (1)$$

One can then assume that the wave function takes the general form of

$\psi = A \exp[i\alpha x] + B \exp[-i\alpha x]$, where $\alpha = [\frac{2m}{\hbar^2}E]^{1/2}$.

2. Materials and methods

Determination of the constants A and B can be achieved by application of the boundary conditions. At $\chi \le 0$ or $\chi \ge a$ the wave function must be zero ($\psi = 0$). Therefore, $0 = A \exp[0] + B \exp[0]$ which simplifies to $A = -B$. In the same fashion, at $\chi = a$, the wavefunction must also be zero, and therefore $0 = A \exp[i\alpha a] + B \exp[-i\alpha a]$. Using $A = -B$ and Euler's formula this can be simplified to $0 = 2Ai \sin \alpha a$, where

we find that αa has infinitely many discrete solutions as

$$\alpha a = n\pi; n = 0,1,2,3 \qquad (2)$$

$$\alpha = \frac{n\pi}{a}; n = 0,1,2,3 \qquad (3)$$

Substituting $\alpha = [\frac{2m}{\hbar^2}E]^{1/2}$ into Eq. 3 gives discrete energy values of

$$E_n = \frac{\hbar^2\pi^2}{2ma^2}n^2; n = 1,2,3 \qquad (4)$$

where the wave function is

$$\psi(x) = \sin(\frac{n\pi}{a}x); n = 1,2,3 \qquad (5)$$

Figure 2. 1a plots the discrete wavefunctions from Eq. 5 while Figure 3. 2b plots the discrete energy levels from Eq.4.
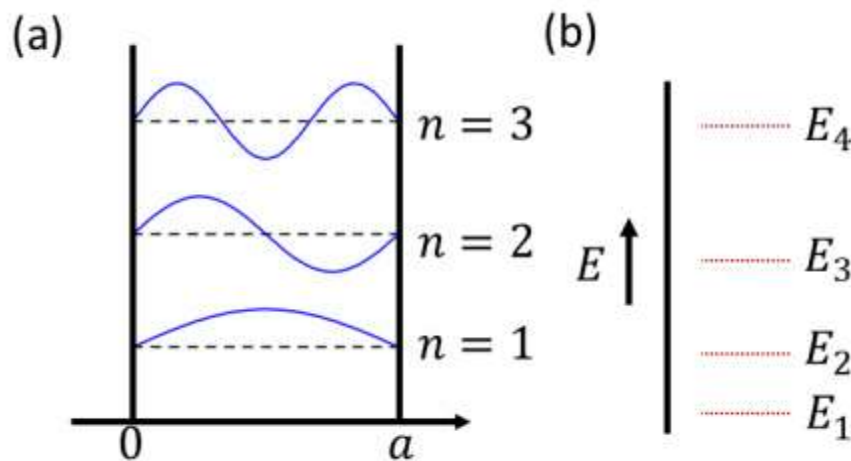
Figure 2. The solution to the particle-in-a-box model results in $a(a)$ simple sinusoidal wavefunction and (b) discrete energy levels.

From this model, we see two intriguing properties. Firstly, the discretization of the energy levels shows that there are certain energies that are forbidden to the electron. Secondly, we see that there is a quadratic relation between the energy and the size of the box (Eq.4). This can be applied to a quantum dot, where the band gap quadratic ally increases as the size of the Nano crystal decreases.

3. Results and discussion

Although the previous model does a reasonable job of identifying the quadratic size dependence of the band gap in quantum dots, the discrete nature of the energy levels is more suitable for atomic electronic structure. The band structure of quantum dots can be more appropriately described using the Kronig-Penney model, which models an electron in a periodic potential, much like it would experience in a crystalline solid (Figure 3). Now in this case the potential is a constant value, $V = V_o$, and there are two diff erent regions for the Schrödinger equation to be applied. The first periodic region has a width of b and is blue in Figure 3, while the second region is the space in between the potentials with a width of a. The Schrödinger equation for these two regions are given in Eq.6 and Eq. 7, respectively, where $\alpha = [\frac{2m}{\hbar^2}E]^{1/2}$

and $\gamma^2 = \frac{2m}{\hbar^2}(V_o - E)$.

$$\frac{d^2\psi}{dx^2} + \frac{2m}{\hbar^2}(E - V_o)\psi = 0 \qquad (6)$$

$$\frac{d^2\psi}{dx^2} + \frac{2m}{\hbar^2}E\psi = 0 \qquad (7)$$

Following a procedure similar to that in Chapter 4, Section 4 of the text Electronic Properties of Materials" by Humme1 and using Bloch functions of the form $\psi(x) = u(x) \exp[ikx]$, one can arrive at

$$P\frac{\sin(\alpha a)}{\alpha a} + \cos(\alpha a) = \cos(ka) \qquad (8)$$

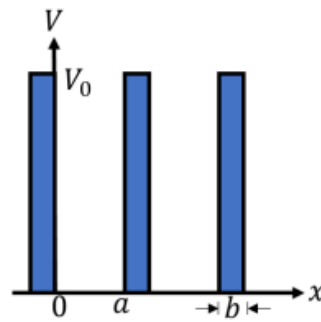where

$$P = \frac{maV_o b}{\hbar^2}. \qquad (9)$$

Figure 3. Periodic potential model.

In this case one again finds discrete solutions to αa, as in the previous example, and in order to better understand Eq. 8 we plot the left -hand side as a function of αa in Figure 3. 4a. Now, because $-1 < \cos(ka) < 1$ we know that for Eq. 8 to hold, $P\frac{\sin(\alpha a)}{\alpha a} + \cos(\alpha a)$ must also be between -1 and 1. The possible values of αa are colored blue in Figure 3. 4a and the possible energy levels according to Eq. 6 and Eq. 7 are plotted in Figure 3. 3b. In a similar fashion to the discrete energy levels from the particle-in-a-box model, one can see that the energy bands increase in a quadratic fashion. Though, unlike the particle-in-a-box, energy bands as opposed to energy levels are now present, which more accurately describes the electronic structure in a quantum dot.
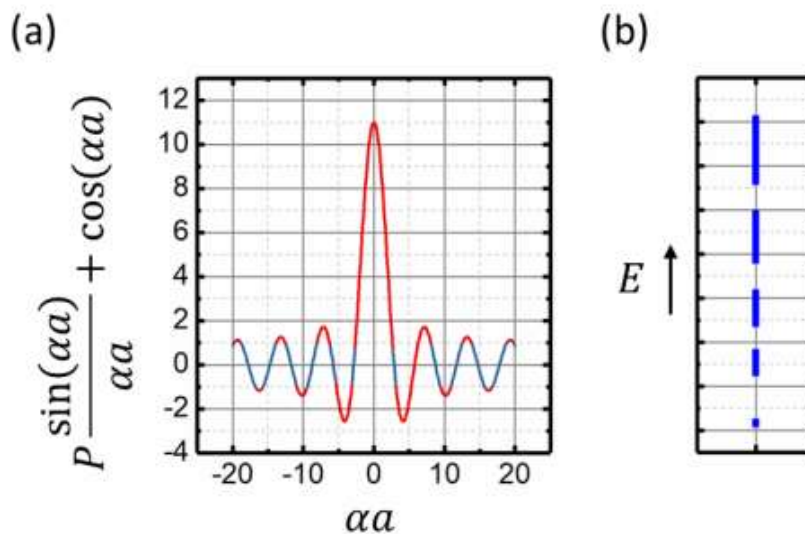

Figure 4. (a) The function $P\frac{\sin(\alpha a)}{\alpha a} + \cos(\alpha a)$ versus αa, where any value of this function that is between -1 and 1 is plotted in blue. (b) Energy bands form from this periodic potential model.

In 1929, three years after the derivation of the Schrödinger equation, Paul Dirac noted that, "The general theory of quantum mechanics is now almost complete . The underlying physical laws necessary for the mathematical theory of a large part of physics and the whole of chemistry are thus completely known, and the difficulty is only that the exact application of these laws lead to equations much too complicated to be soluble. It therefore becomes desirable that the approximated practical methods of applying quantum mechanics should be developed. This is stated because the previous

examples show examples of quantum mechanics being applied to a system with an exact solution as the result. Although this is useful for qualitative analysis and understanding, very few practical cases, as Dirac pointed out, have such simple solutions. Simply increasing the number of electrons from one to two greatly increases the complexity of the calculation. This section will briefly examine the modeling of helium-like atoms using simple approximations of the wave function to discuss the more complex methods used to computationally determine the electronic structure.
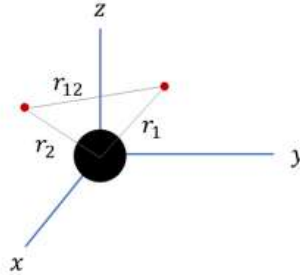

Figure 5. The coordinates of a helium atom with the nucleus at the origin.

Increasing the number of electrons surrounding the nucleus of an atom greatly increases the complexity of the Hamiltonian due to the increased number of electron-nucleus interactions and electron-electron interactions, making these calculations impossible to solve analytically. In the case of helium like atoms with a Hamiltonian of $\widehat{H} = -\frac{\hbar^2}{2m_e}(\nabla_1^2 - \nabla_2^2) - \frac{1}{4\pi\varepsilon_0}\left(\frac{Ze^2}{r_1} + \frac{Ze^2}{r_2} - \frac{e^2}{r_{12}}\right)$ where r_1, r_2, and r_{12} correspond to the distances between electrons and the nucleus per Figure 5, a few approximations can be taken to calculate the wave functions and corresponding energies levels. Such approximations include ignoring the electron-electron repulsion term, $\frac{e^2}{4\pi\varepsilon_0 r_{12}}$, and approximating the wave function as the product of two ls orbitals, $\psi = \frac{1}{\pi^{1/2}}(\frac{Z}{a_0})^{s/2}e^{-Zr_1/a_0}\frac{1}{\pi^{1/2}}(\frac{Z}{a_0})^{s/2}e^{-Zr_1/a_0}$ without concern for spin. These approximations can give reasonable calculations to the total energy of the helium atom at $-74.8eV$ when compared to the exact value of $-79.0eV$. The approximation accuracy can be increased by adding higher order hydrogen orbitals such as the $2p$, $3p$, and $3d$ orbital or by using the variational method.
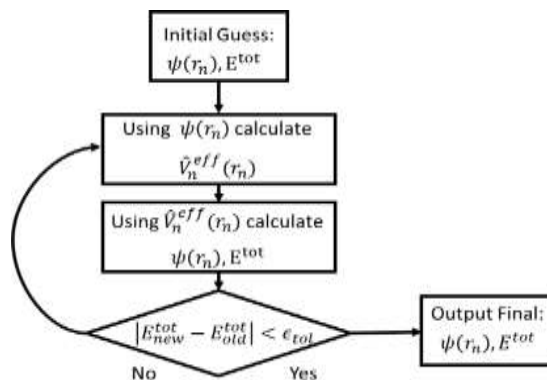
4. Conclusions

Figure 6. Algorithmic flow chart for the Hartree-Fock Method.

For systems with more than two electrons, the approximations used for calculating the total energy in the heliumlike atom also become too impractical. Because of this, the self-consistent field (SCF) method was introduced by Hartre. In this method an effective Hamiltonian, $\hat{H}$, is developed for each electron, n, in the system. This electron only feels an effective averaged potential, $\hat{V}$, from the other electrons resulting in a Hamiltonian as such: $\hat{H} = -\frac{\hbar^2}{2m_e}\nabla_n^2 - \frac{1}{4\pi\varepsilon_0}\frac{Ze^2}{r_n} + \hat{V}(\hat{r})$ The Schrödinger equation for an n-electron atom can now be separated into n one-electron equations which are solved using the SCF method outlined in Figure 3.6. First an approximation of the electronic wave function is made. This wave function is then used to calculate the effective potential where this effective potential is then used to calculate a new wave function. If the difference between the eigenenergies of the new and old wave functions is below the given tolerance, the new wavefunction and its corresponding eigenenergies give the desired output. This is the basis for the Hartree-Fock (HF) method. For a more accurate description of the electronic structure of a system, more advanced computational methods that include exchange correlation functions can be used, such as DFT. DFT builds upon the HF method by

including an approximate treatment of the correlated motions of electrons and has been proven to be very practical in calculating the electronic structure of molecules and materials. In the chapters to follow, many of the experimental data is corroborated with computational simulations using DFT.

REFERENCES:

1. Awschalom, D. D., L. C. Bassett, A. S. Dzurak, E. L. Hu, and J. R. Petta (2013). "Quantum Spintronics: Engineering and Manipulating Atom-Like Spins in Semiconductors". Science 339,1174-1179 (cited on page 8).

2. J. M. Martinis (2013). "Coherent Josephson Qubit Suitable for Scalable Quantum Integrated Circuits". Phys. Rev. Lett. 111, 080502 (cited on page 83).

3. Bennett, C. H. and G. Brassard (1984). "Quantum cryptography: Public key distribution and coin tossing". Proc. IEEE Int. Conf. Computers, Systems and Signal Processing, 175-179 (cited on page 12).

4. Prober, R. J. Schoelkopf, S. M. Girvin, and M. H. Devoret (2010). "Phase-preserving amplification near the quantum limit with a Josephson ring modulator". Nature 465, 64-68 (cited on page 64).

5. Arabboyevich, M. I. (2023). MAGNIT MAYDONDAGI ELEKTRONLAR HARAKATI, LANDAU KVANTLASHISH SHARTLARI. SUSTAINABILITY OF EDUCATION, SOCIO-ECONOMIC SCIENCE THEORY, 1(6), 20-24.

6. Arabboyevich, M. I., & Alijon o'g'li, M. A. (2023). IDEAL GAZLARDA KVANT STATISTIKASI TAHLILI. PEDAGOGICAL SCIENCES AND TEACHING METHODS, 2(20), 235-237.

7. Muminov, I. A., & Muminova, M. (2023). QATTIQ JISMLARNING KRISTALL PANJARALARI. Oriental renaissance: Innovative, educational, natural and social sciences, 3(3), 1314-1317.

8. Arabboyevich, M. I., & Nabijon o'g, S. U. B. (2022). QATTIQ JISM KRISTALLARINI O'STIRISH NAZARIYASI. *Scientific Impulse*, *1*(3), 696-698.

9. Mo'minov, I., & Jasurbek, T. (2022). NAZARIY MEXANIKANING TARIXI. *IJODKOR O'QITUVCHI*, *2*(19), 601-605.

10. Ахмедов, Б. Б., Муминов, И. А., & Хошимов, Х.А.У. (2022). РАЗМЕРНОЕ КВАНТОВАНИЕ В ПОТЕНЦИАЛЬНОЙ ЯМЕ ПРЯМОУГОЛЬНОЙ ФОРМЫ. *Oriental renaissance: Innovative, educational, natural and social sciences*, *2*(Special Issue 4-2), 1032-1036.

11. Muminov, I. A., Axmedov, B.B.,&Maxmudov, A. A. O. G. L. (2022). YARIMO'TKAZGICH ASOSIDAGI TURLI STRUKTURALI NANOTRUBKALAR. *Oriental renaissance: Innovative, educational, natural and social sciences*, *2*(4), 517-523.

12. Baxromovich, A.B.,& Alijon o'g'li, M.A.(2022). YARIMO'TKAZGICH ASOSIDAGI TURLI STRUKTURALI NANOTRUBKALAR Muminov Islomjon Arabboyevich.

13. Muminov, I. A., Akhmedova, S.Y.K., Sobirjonova, D.A.K., & Khomidjonov, D. K. U. (2021). HETEROSTRUCTURES OF ANTIMONIDE-BASED SEMICONDUCTORS. *Oriental renaissance: Innovative, educational, natural and social sciences*, *1*(11), 952-959.

14. Rasulov, R. Y., Akhmedov, B. B., Muminov, I. A., & Umarov, B. B. (2021). Crystals with tetrahedral and hexagonal lattices. *Fergana. Classic.-2021*.

15. Расулов, В. Р., Расулов, Р. Я., Муминов, И. А., Эшболтаев, И. М., & Кучкаров, М. (2021). МЕЖДУЗОННОЕ ТРЕХФОТОННОЕ ПОГЛОЩЕНИЕ В INSB.

16. Ахмедов, Б. Б., & Муминов, И. А. (2021). УРАВНЕНИЯ ШРЕДИНГЕРА ДЛЯ ДВУМЕРНОГО ВОЛНОВОГО ВЕКТОРА. *EDITOR COORDINATOR*, 537.

17. Rasulov, V. R., Akhmedov, B. B., & Muminov, I. A. (2021). Interband one- and two-photon absorption of polarized light in narrow-gap crystals. *Scientific-technical journal*, *4*(1), 28-31.

18. Yavkachovich, R. R., Ogli, M. A. A., Umidaxon, R., Makhliyo, M., & Arabboyevich, M. I. (2019). Agency of surface recombination on volt-ampere characteristic of the diode with double injection. *European science review*, (11-12), 70-73.